

Evaluation of Crop Water Requirements
estimated from Sentinel 2 MSI and Landsat 8 OLI Earth
Observation data in MOSES DSS

Evaluation of Crop Water Requirements

estimated from Sentinel 2 MSI and Landsat 8 OLI Earth
Observation data in MOSES DSS

By

Konstantinos Vlachos

Master of Science

Geoscience & Remote Sensing
Delft University of Technology
Additional Thesis Project [AES4011-10]

Assessment committee: Postdoc dr. Silvia Maria Alfieri, TU Delft
Prof. dr. Susan Steele-Dunne, TU Delft
Prof. dr. Massimo Menenti, TUDelft

An electronic version of this thesis is available at <http://repository.tudelft.nl/>.

*"It is possible to commit no mistakes and still lose.
That is not a weakness.... That is life."*

Captain Jean-Luc Picard

Preface

The current additional thesis project determines a notable landmark during my MSc. studies which brings me a lot more close to the end goal of the last 2 years. In the first place, this project would not be possible to be realized without the assistance and guidance of dr. Roderik Lindenbergh who gave me some ideas and initially introduced me to the topic. In addition, I thank dr. Susan Steele-Dunne and dr. Massimo Menenti for willing to participate in the assessment committee. Of course, I would also like to express my deep gratitude to dr. Silvia Maria Alfieri who was my daily supervisor and assisted and supported me throughout the project by providing me with information and data, face to face and distance discussions, as well as crucial guidance in the right moments. I would say that our collaboration was beneficial which gave me a further good insight about the research process and the role of teamwork, equality and guidance in them. Last but not least, firstly, it would not be possible to even be in TU Delft without the psychological and financial support of my whole family and, secondly, the support and patience of my partner Vasiliki was invaluable, and thirdly, my friends in Delft and especially Kostas who is always there for support the whole time.

In conclusion, I am thankful that through this project I had the chance to detect several faults in terms of how I work, get organized and manage resources (e.g. material, time etc.) which I will have the chance to focus on and get better during my MSc. graduation thesis.

*Kostas Vlachos
Delft, August 2018*

Abstract

MOSES DSS web-platform aims to assist stakeholders such as governments and farmers in order to manage water irrigation distribution in a higher efficiency and sustainability. The constructed algorithms are focused on forecast using weather models, data, as well as satellite multispectral observations in such a way that a 7-day ahead crop water requirement estimation is generated. The current drawback of the system in using the available and free satellite products such as Landsat 8 and Sentinel 2, is that it assumes that the crops are under standard conditions, e.g. there is no water stress, diseases etc.. The current work investigates how possible errors due to this assumption can be potentially tackled in the future by comparing CWR with S2REP VI and/or with water stress index and see the discriminative power of the latter. Furthermore, a comparison between several discrepancies between S2 and L8 (e.g. AC and co-registration) are studied since it is a crucial issue especially in temporal applications such as MOSES. On the one hand, the results showed that a harmonization of the two products is certainly needed. On the other hand, it seems that S2REP is capable of revealing crop stress information based on the methodologies of this work, thus it could potentially give more information compared to NDVI which is not sensitive to crop stress.

Keywords: MOSES DSS, Landsat 8, Sentinel 2, Crop Water Requirement, crop stress, S2REP

List of Abbreviations, Acronyms and Symbols

S2	Sentinel 2
MSI	Multispectral Instrument
L8	Landsat 8
OLI	Operational Land Imager
TIRS	Thermal Infrared Sensor
LaSRC	Landsat 8 Surface Reflectance Code
NIR	Near Infrared
SWIR	Shortwave Infrared
NDVI	Normalized Difference Vegetation Index
S2REP	Sentinel 2 Red Edge Position
CSI	Canopy Stress Index
BI	Bare-Soil Index
CWR	Crop Water Requirement
K_c	Crop Factor
K_s	Crop Stress factor
ET	Evapotranspiration
ET_0	Reference crop Evapotranspiration
ET_c	Crop Evapotranspiration
ET_c^{Adj}	Adjusted Crop Evapotranspiration
RS	Remote Sensing
EO	Earth Observation
DEM	Digital Elevation Model
SRTM	Shuttle Radar Topography Mission
L1C	Level 1C
L2	Level 2
VPD	Vapor Pressure Deficit
LST	Land Surface Temperature
T_c	Canopy Temperature
T_a	Air Temperature
ϵ	Emissivity
λ_c	Central wavelength
T_B	Brightness Temperature (K)
h	Planck's constant
σ	Boltzmann's constant
c	Speed of light in space
LAI	Leaf Area Index
LCC	Leaf Chlorophyll Concentration
AC	Atmospheric Correction
TOA	Top-Of-Atmosphere
SNAP	Sentinel Application Platform
EPSG	European Petroleum Survey Group
QA	Quality Assessment
UTM	Universal Transverse Mercator
CRS	Coordinate Reference System
LUT	Look-Up-Table
DSS	Decision Support System
BRDF	Bi-directional Reflectance Distribution Function
MODTRAN	MODerate Resolution Atmospheric Transmittance
WDVI	Weighted Difference Vegetation Index
MOBAC	MODtran Based Atmospheric Correction
KNN	K-Nearest Neighbor
SW	Shortwave
LW	Longwave
RSEB	Remote sensing Surface Energy Balance

Contents

Abstract	v
1. Introduction.....	1
1.1. Motivation and purpose.....	1
1.2. CWR theoretical background.....	1
1.3. Research Questions	3
1.4. Study Area	3
2. Materials and Methods	5
2.1. Category (a)	6
2.2. Category (b)	6
2.3. Category (c)	7
2.4. Vegetation Indices (VIs).....	8
2.5. Crop Water Requirement	9
2.6. Canopy Stress Index (CSI)	9
2.7. Bare-Soil Index (BI)	11
3. Results and Discussion	12
4. Conclusions and Suggestions.....	17
5. References	19
6. Appendix.....	22

1. Introduction

1.1. Motivation and purpose

This work is a minor part in the framework of the MOSES (Managing crOp water Saving with Enterprise Services) project which in turn operates under the umbrella of the research and innovation European programme H2020 being a DSS. The MOSES project aims to put in place and demonstrate at the real scale of application an information web platform devoted to water procurement and management agencies. The platform will provide information and support to water management authorities and farmers in order to make more efficient and sustainable use of water resources in agricultural activities. Ideally, the above stakeholders should be staying up-to-date by being provided with crop status information regularly. One of the main system components of the MOSES platform is the in-season monitoring and short term forecast of Crop Water Requirement (CWR)¹. Monitoring and short term forecast of CWR at high temporal resolution can be realized by using a combination of weather observation data and forecast models as well as multispectral Earth Observation (EO) data. Currently, MOSES platform does not provide sufficient prediction in the case when crops undergo stress, i.e. water, salinity. The purpose of this project is to investigate the quality of the EO data outputs after processing, as well as make them more informative. More information can be found on the relevant webpage (http://moses-project.eu/moses_website/) as well as in Di Felice et al. (2017).

1.2. CWR theoretical background

One significant process in the general water balance model, along with runoff, precipitation and infiltration, is the evapotranspiration (ET). Generally, water transits from liquid to the gaseous phase through the evaporation from the soil, as well as the transpiration from the vegetation.

According to the guidelines provided by the Food and Agriculture Organization of the United Nations (Allen et al., 1998) the ET in an agricultural domain depends on three factors; weather (radiation, air temperature, wind speed, humidity), environmental conditions including human factor (e.g. soil water content, soil permeability, diseases etc.) and crop factors (crop type, variety and growth stage). The crop ET under ideal climatic conditions can be defined as the reference crop ET (ET_0) which assumes grass as a reference crop. Making the model more realistic, a crop factor K_C is incorporated which represents the accumulated crop characteristics, thus the new ET is defined as ET_C considering ideal environmental conditions. In addition, considering that environmental conditions are not perfect, we arrive at the final adjusted form of ET, $ET_{C,adj}$ which includes a crop water stress factor (K_S). Eventually, taking into account the above information and under the context of the current project the CWR can be defined as the amount of water that is

¹ See definition in Section 1.2.

necessary in order to compensate for the water decrease due to ET_c , thus the water needed for the crop to grow optimally. The crops are considered to be under standard non-stressed condition.

Remote Sensing approach

In the case of EO data the aim is to use Landsat 8-OLI (L8) in combination with Sentinel-2 MSI (S2) missions, since they provide free online access and they can result in higher temporal resolution if used together. Namely, the temporal resolution of L8 is 15 days (U.S. Geological Survey, 2016), while for S2 constellation is 5 days, at the equator (ESA, 2015). However, the temporal resolution is even greater for both satellites at the mid latitudes, because of adjacent swath overlap, among others. In the study area which is presented later, L8 and S2 temporal resolution lies between 7-9 days and 2-3 days, respectively, which can give a final temporal resolution of 1-3 days. The full potential of a minimum timespan of 1 day between some acquisitions can only be gained under cloud-free conditions, although an even lower temporal resolution of e.g. 2-3 days will be adequate in the case of atmospheric noise such as clouds.

The RS application in estimating CWR has been mainly focused on three approaches; (i) RSEB (ii) crop coefficient and (iii) Penman-Monteith equation (Akdin et al., 2014; Calera et al., 2017). In order to estimate the CWR using RS, it has been shown that certain spectral regions are mainly useful which are exploited using vegetation indices, which in turn are correlated with crop parameters such as chlorophyll content, nitrogen content, biophysical etc. (Akdin et al., 2014). With regard to L8 and S2 instrument payload specifications they show lots of similarities since S2, at its core, was designed to provide continuity to Landsat series, among others. A comparison of the spectral resolution and bands can be seen below (Fig. 1). In particular, the bands that are used commonly in the CWR estimation are the red and NIR whose comparison between the two satellites can be seen in Table 1. The band 8a (20 m spatial resolution) of S2 is an equivalent to band 8 (10 m) and Landsat's band 5, and was designed in order to minimize water vapor noise that Landsat experience showed to be apparent (U.S. Geological Survey, 2016).

Table 1. Landsat 8-OLI and Sentinel 2-MSI bands that are commonly related to CWR estimation, as well as the red edge region bands of the S2

Satellite	Band Name/Number	Central Wavelength (nm)	Bandwidth (nm)	Spatial Resolution (m)
Landsat 8-OLI	Red/4	654.5	37	30
	NIR/5	865	28	30
Sentinel-2	Red/4	665	30	10
	NIR/8	842	115	10
	Narrow NIR/8a	865	20	20
	Red edge 1/5	705	15	20
	Red edge 2/6	740	15	20

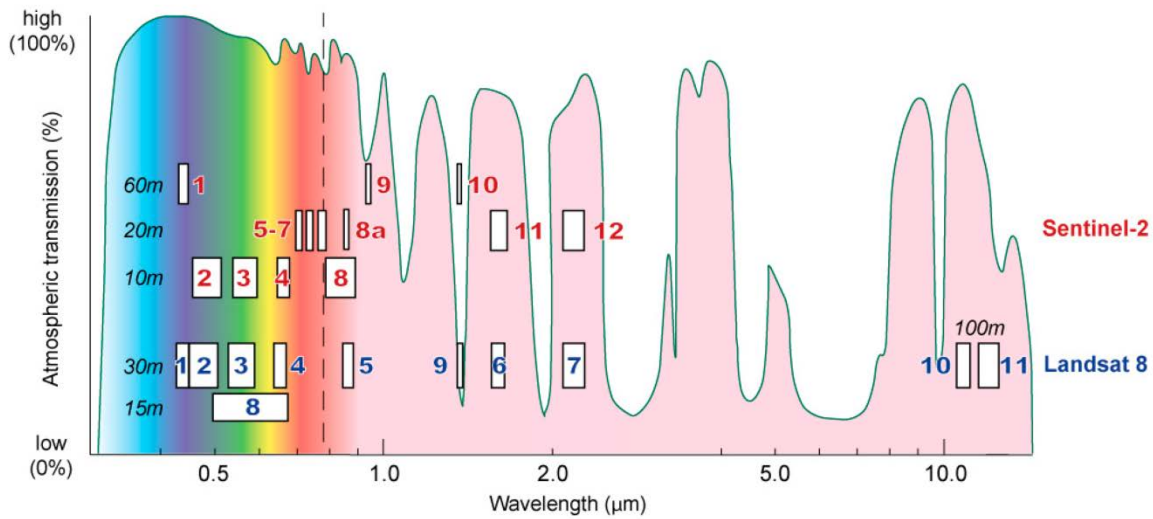


Figure 1. Spectral resolution comparison between Landsat 8 and Sentinel-2 (from Kääb et al., 2016)

1.3. Research Questions

The two main research questions to be answered in the current project pertain to:

- i) How and, if so, why Sentinel 2 and Landsat 8 differ in terms of estimating crop water requirement
- ii) How good or bad is the use of kc-NDVI method (D’Urso, 2010) in estimating crop water requirement taking into account that in reality there are no standard crop conditions (e.g. crops are under water stress)

In other words, the first goal of this study is to assess the potential differences between S2 and L8 in estimating CWR and the second is whether crops under non-standard conditions can be identified using red edge position (S2REP) and canopy temperature (CSI) based indices, since NDVI is not sensitive enough.

1.4. Study Area

In MOSES project four demonstration areas have been set up; Italy, Spain, Romania and Morocco. The current thesis work is focused on the demonstration area in Italy (Fig. 2) which is located in a relatively flat area which comprises the irrigation districts. Namely, the wide majority of the region where the different plots are placed is characterized by very small slopes (< 3.8°) as inspected by deriving the slope of the 1-arcsec Digital Elevation Model (DEM) of Shuttle Radar Topography Mission (SRTM) (Fig. 3). Its climate is continental (summer maximum temperatures above 30 °C), mitigated by sea influence in the North-eastern part. The Apennine mountains on the Eastern side cause instability generating hot dry spells, with prevailing south-west currents,

mainly in Winter and Springs, and strong rainfall events, with prevailing Eastern currents. Although the total amount of rainfall appeared to be stable (750-850 mm), during the last few years a change of the temporal distribution has been recorded, namely an increase of heavy rainfall events alternated with long periods of drought is being realized.

The Total Agricultural Surface in the area is about 230000 ha where approximately 16000 farms are operating. The 70% of the Used Agricultural Surface (about 165000 ha) is dedicated to the cultivation of sown crops and the 20% to the agricultural woody plants, while the prevailing crops are wheat, meadow, alfalfa, maize, sorghum, peach, vineyard, horticulture and sugar beet (2015 AGREA data).



Figure 2. MOSES demonstration area in Italy bounded by the intermittent white line.

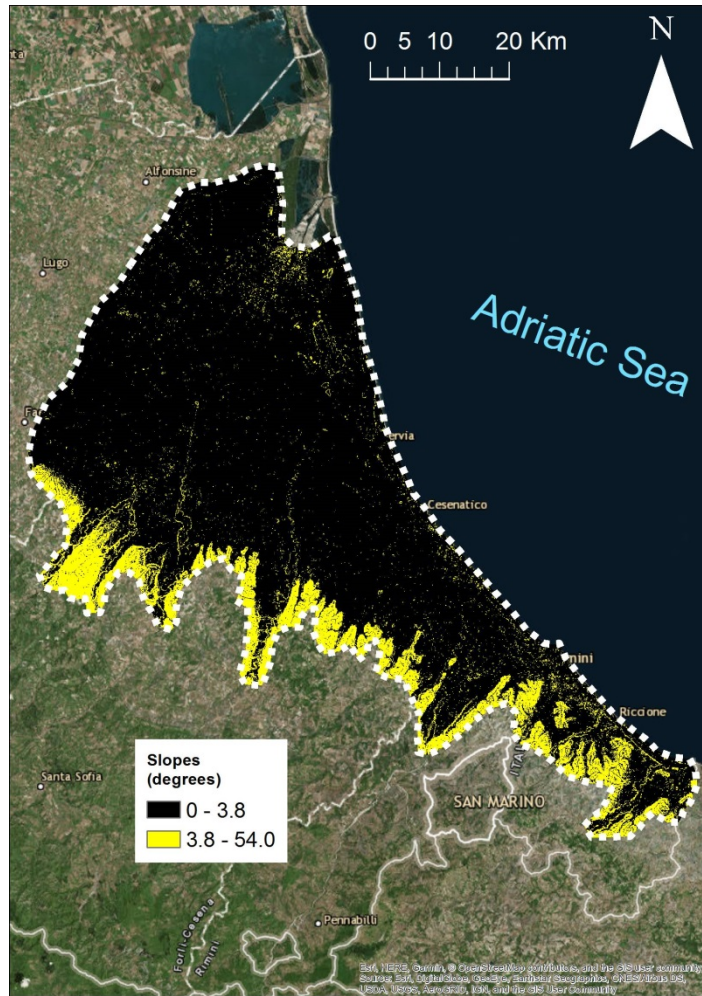


Figure 3. The slopes (in degrees) of the morphological relief of the study area in Italy. The slopes have been generated by using the SRTM DEM (1-arcsec).

2. Materials and Methods

The datasets used can be classified into four categories; (a) L2 for L8 OLI and S2 MSI (b) L1 for L8 OLI/TIRS and S2 MSI and (c) miscellaneous. All three of them are described thoroughly below. Regarding (a) and (b) the satellite images of S2 and L8 that were used in this project were downloaded directly from the corresponding web platforms that are scihub.copernicus.eu/dhus/#/home and earthexplorer.usgs.gov/, respectively. The former's CRS is by default WGS84/UTM zone 32N (EPSG: 32632) while the latter's is WGS84/UTM zone 33N (EPSG: 32633). Every processing step was accomplished using ArcGIS™ benefitting from ModelBuilder and ArcPy, Python, MATLAB™, SNAP benefitting from the iCOR plugin (Sterckx et al., 2015a) and QGIS benefitting from the Semi-automatic classification plugin (Congedo, 2016). With regard to the co-registration procedure, it has been observed that S2 and L8 are not completely aligned due to some errors in the ground stations of L8 (Claverie et al., 2017). This is the reason that several preliminary procedures were realized (see Appendix).

2.1. Category (a)

Table 2 shows the ID information of the tiles of both satellites. As for S2, two scenes were downloaded which slightly overlap. The date of acquirement is 20/06/2017 and the time ~ 09:52 and ~10:00 for L8 and S2, respectively. This is a fact that minimizes any discrepancies pertaining to solar angles etc. In addition, the L2 of L8 is an on-demand product, which means that the user needs to wait for several hours or maybe 1 day to have it delivered. S2 is generated using the sen2cor AC algorithm whilst L8 using LaSRC algorithm (Vermote et al., 2016).

Table 2. The Scene ID information regarding L8 and S2 L2 products as provided by the relevant services (NASA, ESA).

Landsat 8	LC08_L1TP_191029_20170620_20170630_01_T1
Sentinel 2	S2A_MSIL2A_20170620T100031_N0205_R122_T32TQP_20170620T100453 S2A_MSIL2A_20170620T100031_N0205_R122_T32TQQ_20170620T100453

Pre-processing

The L2 products can directly provide information, such as the land cover, cloud coverage, saturated pixels, probable sensing issues etc. Therefore in this preliminary step of quality assessment the *Landsat QA ArcGIS Tools* toolbox was used in order to decode the corresponding QA bands of L8, such as LC08_L1TP_191029_20170620_20170630_01_T1_pixel_qa.tif, LC08_L1TP_191029_20170620_20170630_01_T1_radsat_qa.tif and LC08_L1TP_191029_20170620_20170630_01_T1_sr_aerosol.tif. The quality of every parameter seems to be adequate (e.g. sun elevation angle not too low (~64°)), as well as the cloud coverage over land was at minimal levels (0.11 %). Same thing holds for the aerosol presence which was high just over the towns which do not affect further processing since it is focused over the crops. Same procedure was followed for S2, where the saturation of pixels was minimal, thus do not affect the processing.

Next step was to rescale the pixel values based on the rescaling factor 0.0001. Furthermore, a mosaic regarding S2 two different tiles of the scene of interest was created. This was realized using nearest neighbor interpolation without any feathering or smoothing, thus not affecting the original pixel values. As a last step, the S2 mosaicked scene was co-registered to L8 scene using the SNAP collocation tool. Collocation tool, according to SNAP help documentation, performs an automatic geographic co-registration (alignment-reprojection/resampling) using tie points, although no further information is available.

2.2. Category (b)

Same type of information as in category (a) can be seen in Table 3. Regarding time and date, of course, the same situation holds.

Table 3. The Scene ID information regarding L8 and S2 L1 products as provided by the relevant services (NASA, ESA).

Landsat 8	LC08_L1TP_191029_20170620_20170630_01_T1
Sentinel 2	S2A_MSIL1C_20170620T100031_N0205_R122_T32TQP_20170620T100453 S2A_MSIL1C_20170620T100031_N0205_R122_T32TQQ_20170620T100453

Pre-processing

The preprocessing steps were followed for the L1 products of S2 and L8 tiles. In particular, only the relevant bands that were going to be used for the spectral indices were processed, i.e. B2, B4, B5, B6, B7, B8a, B8, B11 for S2 and B4, B5 for L8.

Following, they were radiometrically and atmospherically corrected using the iCOR algorithm which is provided as a SNAP plugin. iCOR AC scheme is based on MODTRAN-5 LUTs (Berk et al., 2005) and innate band information and it has been especially created in order to harmonize L8 and S2 regarding AC (Sterckx et al., 2015a). The parameters that were used for both S2 and L8 were the default using an adjacency effect correction with an adjacency window of size 3x3. There was no need to apply the SIMEC adjacency correction since it is not necessary to strictly correct over water bodies for which SIMEC is specialized (Sterckx et al., 2015b). The adjacency effect is denoted as the noise of a pixel that originates from the scattering of the adjacent areas (pixels).

After this, the products of each spectral band were co-registered using the collocation tool in SNAP and nearest neighbor resampling (30m) interpolation method. Again, the S2 tiles were mosaicked band by band with the same option as in category (a).

As far as the L8 thermal band (B10) concerned, the processing procedure is described later. In addition, the same procedures were followed for the S2 bands that are relevant to BI except that they were not co-registered and resampled with L8 since there was no need.

2.3. Category (c)

The miscellaneous dataset is composed of rasters such as ET_o , VPD, Air Temperature and crops polygons shapefile, as well as L8 LAI which was provided as an output from the MOSES processing platform. Everything is re-projected to WGS84/UTM zone 33N using nearest neighbor interpolation. The maize polygons are selected and extracted to a separate shapefile out of the crops polygon based on the ID of maize (ISM_ID = 38). Following, the ET_o raster is converted to polygon and in combination with the maize polygon, the maize polygon that are completely within the ET_o polygon are selected and extracted (Fig. 4). The final maize polygon is used as the clip polygon in order to restrict the further processing to maize, which is the crop of interest since it is grown during the month of June. It is worth to note that the crop classification was realized using KNN classifier by MOSES algorithms. The dataset used was a combination of spectral bands of pairs of images with a time lag of 15 days between them. For further information on MOSES crop classification one can refer to Spisni et al. (2017).

The ET_o was computed based on the Penman-Monteith equation (Allen et al., 1998; Akdim et al., 2014) using weather data measured from ground stations as parameters, as well as using crop reference (grass) values. The formula used by MOSES platform can be seen below:

$$ET_c = \frac{1}{\lambda} \frac{\Delta(R_{ns} - R_{nl} - G) + 1.013\rho D_e / r_a}{\Delta + \gamma(1 + r_{c,min} / r_a)}$$

Where:

λ is the latent heat of vaporization [MJ/kg];

R_{ns} is the net SW radiation (MJ/m²d);

R_{nl} is the net LW radiation (MJ/m²d);

G is the soil heat flux (kJ/m²s),

D_e is the VPD of the air (kPa);

ρ is the mean air density at constant pressure (kg/m³);

γ is the psychrometric constant (kPa/°C);

Δ is the slope of the saturation vapour pressure temperature relationship (kPa/°C);

$r_{c,min}$ and r_a are the minimum surface (in the absence of water stress) respectively the aerodynamic resistance.

With regard to L8 LAI, it was produced out of L1 products which were atmospherically corrected using the MOBAC AC scheme developed specifically for MOSES project (Alfieri & Menenti, 2016). MOBAC is based on MODTRAN LUTs. Furthermore, LAI was computed using the procedure that is described by Akdim et al. (2014) which is based on WDWI.

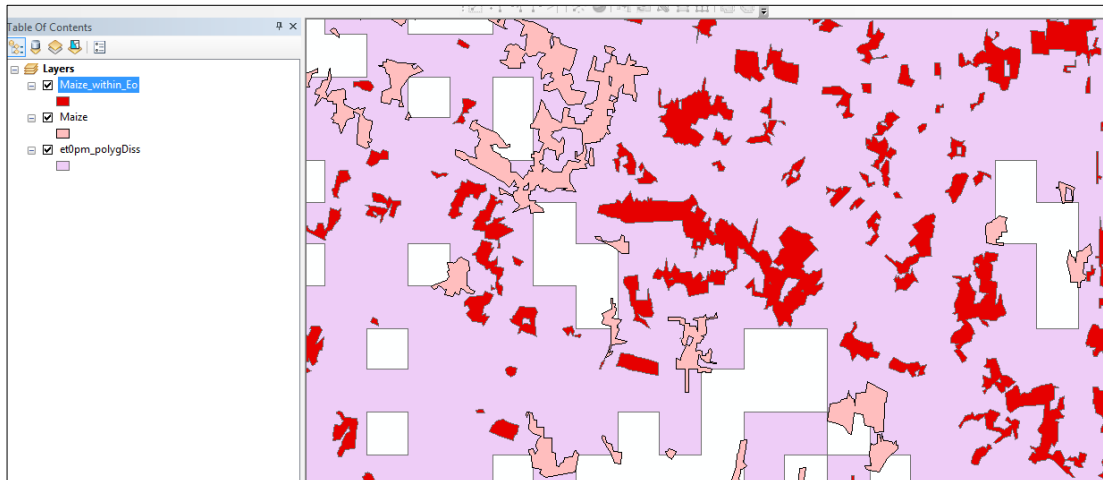


Figure 4. Spatial analysis of maize polygons. The purple polygon represents the ET_o . The red and pink polygons show the maize plots. The red polygons represents those maize polygons that are used in the analysis and calculation of CWR that fall completely within the ET_o polygon.

2.4. Vegetation Indices (VIs)

The Normalized Difference Vegetation Index (NDVI) for Sentinel 2 was computed as below:

$$NDVI = \frac{B8_a - B4}{B8_a + B4}$$

while for Landsat 8 as:

$$NDVI = \frac{B5 - B4}{B5 + B4}$$

The Sentinel 2 Red Edge Position (S2REP) was computed as developed in Frampton et al. (2013) using all three red edge bands and can be seen below:

$$S2REP = 705 + 35 \frac{\frac{B7 + B4}{2} - B5}{B6 - B5} \text{ (nm)}$$

Red edge is the spectral region where plant leaves and canopy reflect light with the largest slope and this is why it is so informative, thus useful for vegetation studies including chlorophyll content estimation (Filella & Penuelas, 1994; Frampton et al., 2013). The reflectance increases from about 0.68 μm to 0.75 μm .

2.5. Crop Water Requirement

Based on Allen et al. (1998) the CWR (or ET_c) is computed through:

$$ET_c = K_c ET_o$$

Using the RS approach the K_c can be computed as (D'Urso, 2010; Rocha et al., 2012; Akdim et al., 2014):

$$K_c = 1.25 NDVI + 0.2$$

The two numerical parameters of the above equation can change locally based on the crop under study (D'Urso, 2010; Rocha et al., 2012), although in the current work the default formula is used.

2.6. Canopy Stress Index (CSI)

The foundation of crop stress index can be found in Idso et al. (1981a) and Idso (1981b) which is based on transpiration which in turn depends on air and canopy temperature as well as vapor partial pressure; the estimation of crop water stress is based on field measurements. However, since remote sensing approach inserts error due to noise Rodriguez et al. (2005) developed a solely satellite remote sensing version of the aforementioned work which is named Canopy Stress Index. CSI is defined as:

$$CSI = \frac{T_c - T_a}{VPD} (^\circ C/kPa)$$

where T_c ($^\circ C$) is the canopy temperature, T_a ($^\circ C$) is the air temperature and VPD is the Vapor Pressure Deficit (kPa) as a normalization factor. Below, the steps towards the CSI computation are described in this project.

Firstly, thermal band (B10) of L8 L1C product was derived in order to compute the Land (or Canopy) Surface Temperature (LST). According to U.S. Geological Survey (2016) thermal Band 11 should be avoided due to very high noise that originates from stray light. The LST is computed using the L8 LAI as derived by the MOSES processing platform (Akdim et al., 2014) as seen below (Weng et al., 2004) using the Semi-automatic classification plugin (Congedo, 2016):

$$LST = \frac{T_B}{1 + \frac{\lambda_c T_B}{\rho} \ln \varepsilon} - 273.15 (^\circ C)$$

where T_B is the Brightness temperature, λ_c (μm) the central wavelength of B10, ε the emissivity and ρ is a product of constants. In particular:

$$\rho = h \frac{c}{\sigma} (\mu m K)$$

where $h = 6.626 \cdot 10^{-34}$ J s (Planck's constant), $c = 2.998 \cdot 10^8$ m s⁻¹ (speed of light in space), $\sigma = 1.38 \cdot 10^{-23}$ J K⁻¹ (Boltzmann's constant)

and

$\lambda_c = 10.895 \mu m$ (B10 central wavelength)

Following, T_B is computed according to U.S. Geological Survey (2016). As a result, a conversion to Top-Of-Atmosphere (TOA) spectral radiance based on the information provided in the metadata (*.MTL) file is needed using:

$$L_\lambda = M_L Q_{cal} + A_L \left(\frac{W}{m^2 \cdot sr \cdot \mu m} \right)$$

where M_L is B10 multiplicative rescaling factor (RADIANCE_MULT_BAND_10), A_L is B10 additive rescaling factor (RADIANCE_ADD_BAND_10) and Q_{cal} is the quantized and calibrated standard product pixel value (Digital Number)

$$\text{and } T_B = \frac{K_2}{\ln\left(\frac{K_1}{L_\lambda} + 1\right)} (K)$$

where T_B is the brightness temperature assuming an emissivity equal to 1, K_1 and K_2 are the thermal conversion constants for band 10 ($Kx_CONSTANT_BAND_10$)

and finally ε = emissivity which can be computed based on LAI as (Allen et al., 2002) and is valid at the areas where NDVI is positive:

$$\varepsilon = 0.95 + 0.01 \cdot LAI, \text{ for } LAI < 3$$

and

$$\varepsilon = 0.98, \text{ for } LAI \geq 3$$

Furthermore, according to Rodriguez et al. (2005) the derived LST is a mixed signal that originates from canopy and soil. Therefore, it should undergo a correction based on the ground cover –equivalent to Fractional Vegetation Cover (FVC). The aforementioned researchers derived empirical relationships between the correction parameter *Delta* and some VIs for wheat crops. In the current work by extrapolation the relationship between *Delta* and NDVI is used on maize crops which is:

$$Delta = 28.4 \cdot e^{-3.6 NDVI} (^{\circ}C)$$

As a result, the final canopy temperature becomes:

$$T_c = LST - Delta$$

Regarding the rest of the two parameters for calculating CSI, namely air temperature (T_a) and VPD they are derived from MOSES platform meteorological inputs. The final product is the CSI raster in 30m spatial resolution which denotes a crop under stress when it is positive and a healthy crop when it is negative.

2.7. Bare-Soil Index (BI)

The Bare-Soil Index was originally developed by Roy et al. (1996) and later reformulated by Roy et al. (1997) and Rikimaru & Miyatake (1997). The index was developed based on Landsat TM and discriminates well between non-vegetation (e.g. bare soil) and sparse or dense vegetation since it uses both absorption and reflectance bands, such as blue, red, NIR and SWIR. In addition, it has also being implemented for Landsat 8 OLI/TIRS (Akike & Samanta, 2016). As a result, in this study the equivalent index in S2 is used below which also offers better spatial resolution (10m) than L8 (30m):

$$BI = \frac{(B_{11} + B_4) - (B_5 + B_2)}{(B_{11} + B_4) + (B_5 + B_2)} \cdot 100 + 100$$

where approximately $0 < BI < 200$; high values denote presence of bare-soil and low values denote dense vegetation.

By taking into account the histogram of the BI it seems to represent a mixture distribution, namely being bimodal. The one mode with the lower values represents the higher vegetated plots of maize while the second mode with higher values represents the less vegetated plots and/or bare soil that may be misclassified as maize. The latter information is an indication that came from visual inspection of the study area where not perfect maize classification was realized. In order to further filter the pixels that are supposed to represent maize in the same development

stage (maximum growth) based on the MOSES in-season crop mapping classification, a decision boundary was chosen over which the values are disregarded. The threshold was chosen by fitting a kernel density function on to the BI histogram values and then considering the local minimum as the decision boundary (Fig. 5). However, since the data showed two local minimums, the one with the highest BI (= 77) was chosen as the threshold value in order to include more values from the first mode (denser vegetation), although importing some noise because of the uncertainty due to mixture distribution and the incorporation of more values of the second mode (less vegetation and/or bare soil).

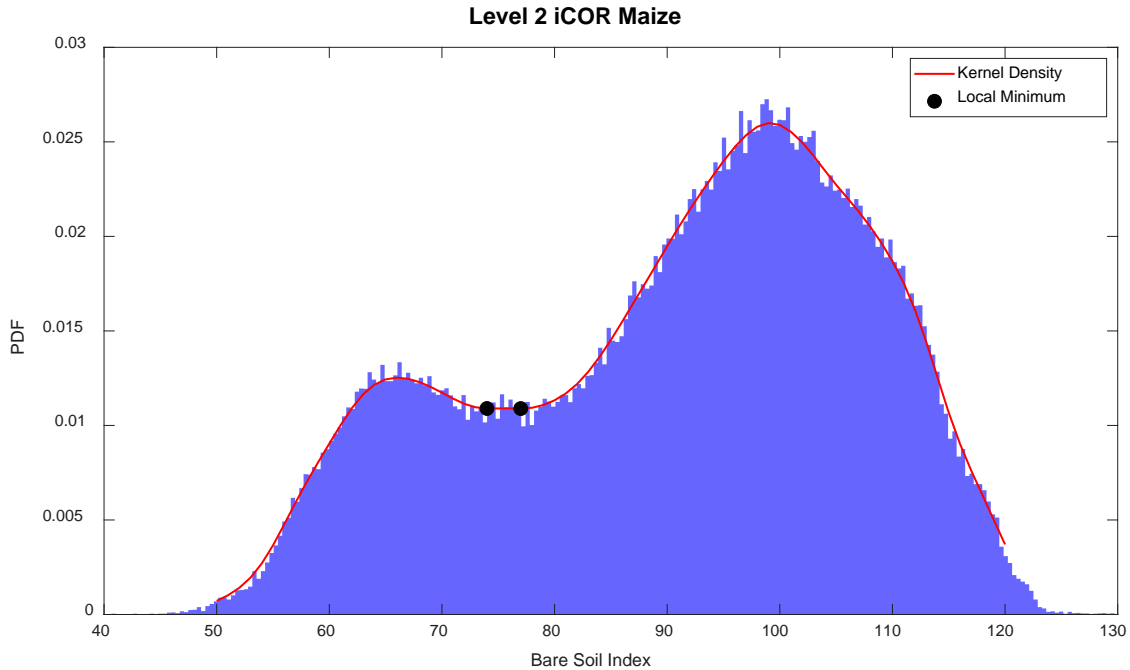


Figure 5: The graph depicts the histogram of the BI generated from S2 relevant bands. It is clearly a mixture distribution, namely bimodal. The mode at the left side represents the maize regions where there is dense vegetation, while the mode at the right side represents those regions that are either sparse vegetation and/or bare soil misclassified as maize.

3. Results and Discussion

As far as the pre-processing stage concerned, several simplifications and assumptions were made for the accomplishment of this thesis. In particular, despite the two satellite sensor differences such as spectral and orbital setup which affect the signal that is received, only the radiometric (partly), atmospheric and geometric correction were taken into account in this work. Thus, there was no such pre-process as BRDF adjustment and/or band adjustment such as those proposed in Claverie et al. (2017) or Zhang et al. (2018) which are used to almost completely harmonize the L8 and S2 sensors. Thus for a completely harmonized comparison between the products one should treat the following information with care.

Regarding the comparison itself between S2 and L8 products, several graphs and comments can be seen in the Appendix. They are not included in the current section since they were out of the initial scope of this study, although the discrepancies between the two satellites were considered significant therefore the comparison of different combinations between AC and co-registration was inevitable in order to choose the best AC and co-registration in the category (b) datasets. Generally, the co-registration is very important in a time series application such as MOSES project thus there are several approaches to solving this issue, namely described by Stumpf et al. (2018), Skakun et al. (2017) and Gao et al. (2009). Furthermore, apart from the misregistration between L8 and S2 due to L8 ground segment issue (Claverie et al., 2017) another geometrical discrepancy has been observed lately in Sentinel 2-A between different dates above the same geographical region (Yan et al., 2018), therefore this could be also an issue that needs care, although this is not an obstacle of the current study.

Category (a)

The results of the NDVI comparison regarding the category (a) can be seen below (Fig. 6a). The relation is linear as expected although it is not 1:1. Furthermore, the histogram along with summary statistics, as well as the absolute difference can be seen (Fig. 6b-d). The central tendency statistical moments are expected to be 0, ideally with a small standard deviation although this is not the case. The largest deviation between the two is observed at the lowest and highest quartiles (Fig. 6b). As is apparent, the L2 products of S2 and L8 provided by the services cannot be used in combination directly as they are –or at least by just simply co-registering– for CWR estimation due to the biasedness and not good agreement. This difference is most likely owed to the differentiation between the two AC schemes that the services use. Further information which elaborate on this can be found in the Appendix graphs which show the discrepancies and their most probable causes better.

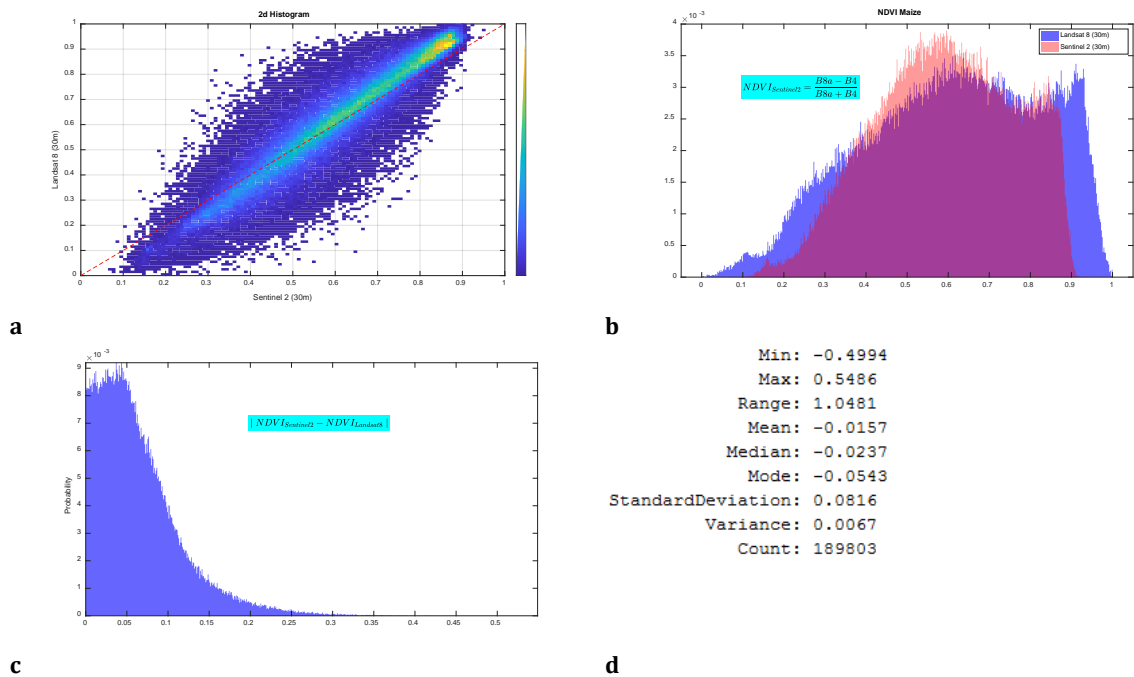
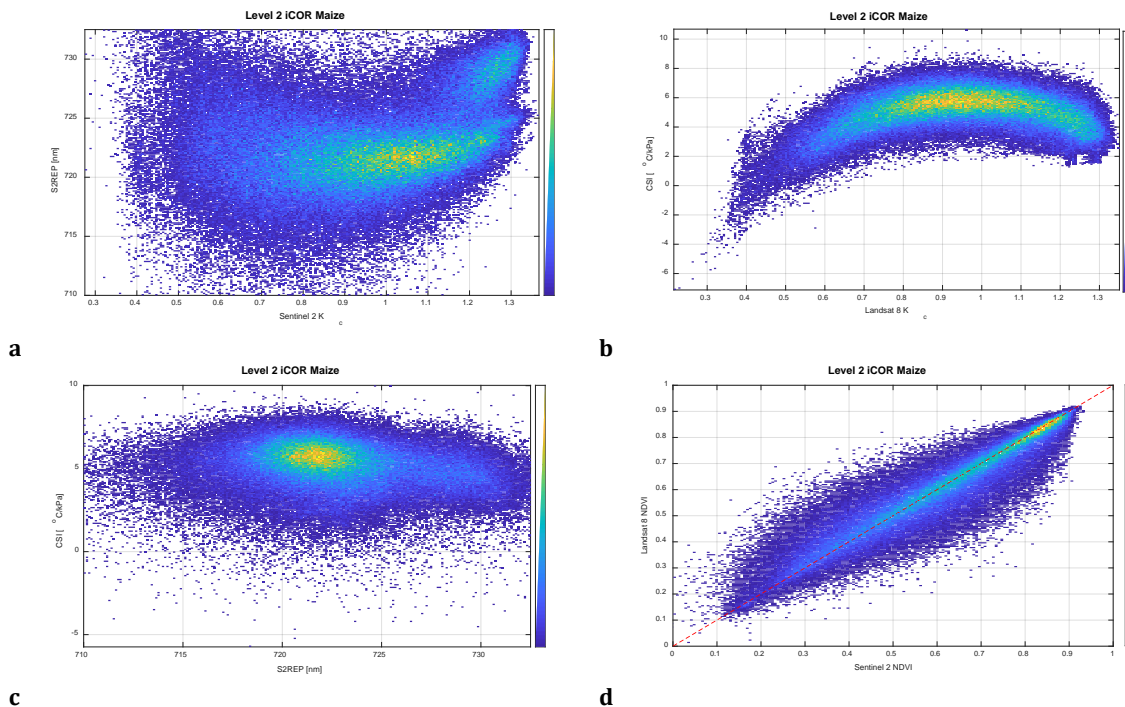
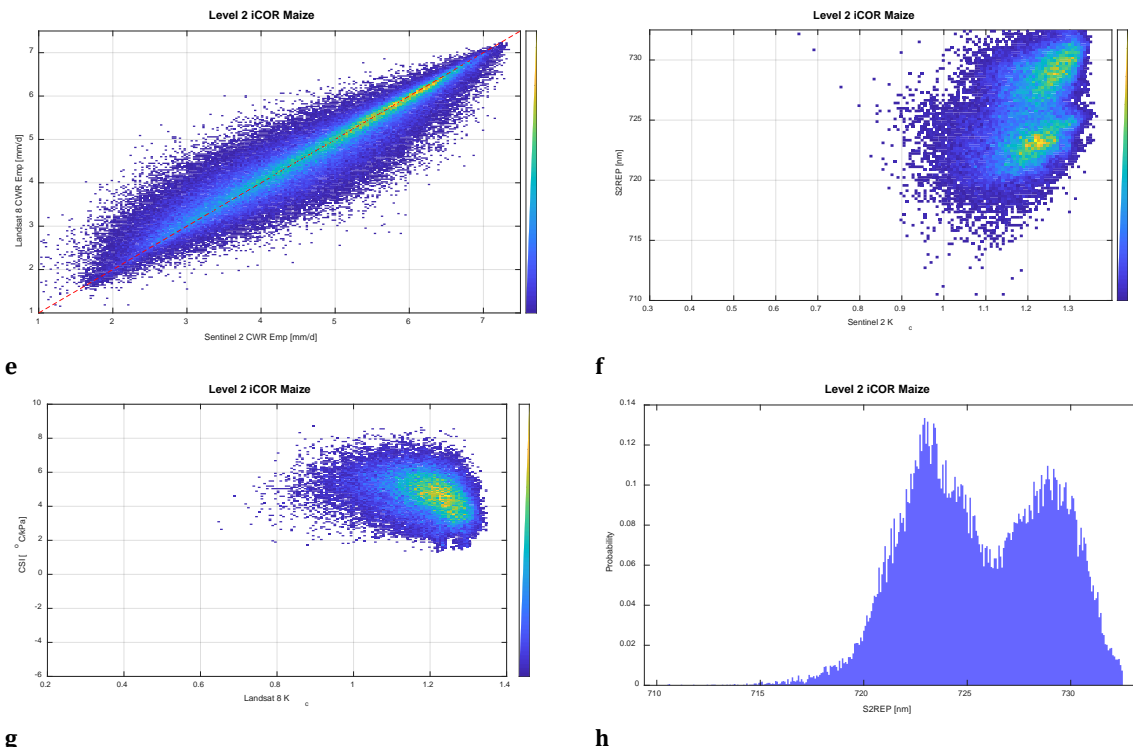


Figure 6: a) Graphs shows the 2D histogram of the S2 vs L8 NDVI as computed by the L2 products downloaded directly from the relevant web services. The red intermittent line represents the 1:1 line b) Histogram of S2 and L8 NDVIs. The S2 histogram is transparent on top of the L8 histogram c) The absolute difference of S2 and L8 NDVIs which should be concentrated on top of 0 but this is not the case d) Summary statistics of the difference of S2 and L8 NDVIs.

Category (b)

The following information concern the category (b) datasets, namely the iCOR atmospherically corrected L1 products. The comparison between S2REP/CSI and K_c (Fig. 7a, b), S2REP and CSI (Fig. 7c), as well as NDVI/CWR L8 and CWR S2 can be seen below (Fig. 7d, e). The comparison of S2REP/CSI with K_c was chosen in order to avoid including the slight effect of ET_0 which would hide some information. First of all, in the graphs S2REP/CSI versus K_c a parabolic shape is observed. The curve starts taking an opposite direction at approximately $K_c=1$ (Fig. 8). By inspecting the map overlaid by BI and looking at the BI histogram there seem to be two modes or regions; one region which is either bare-soil or very sparsely vegetated (maybe crops that are in the beginning of their growth). By using the BI filter the lower values of the variables are disregarded in order to isolate crops at the maximum development stage (Fig. 5). Specifically, the values of K_c lower than ~ 1 are disregarded and the trend that is considered valid is kept. Namely, the positive and negative correlation between S2 K_c -S2REP (Fig. 7f) and L8 K_c -CSI (Fig. 7g), respectively, is an expected result.





g Figure 7: a) Kc-S2REP 2D histogram which show curve that first decreases and then increases. Also there are two modes observed which is probably related to the difference in LCC b) Kc-CSI 2D histogram that shows similar but opposite relation as Fig. 7a c) S2REP-CSI 2D histogram which barely shows a correlation. In fact it is very slight negative if not absent d) Relationship between S2-L8 NDVI produced by iCOR AC and collocation tool co-registration by ESA SNAP. The relationship agrees with the 1:1 red intermittent line e) The corresponding S2-L8 CWR as produced by the NDVI in Fig. 7d using the Kc-NDVI empirical method f) The same graph as Fig. 7a filtered using the BSI = 77 threshold g) Same graph as in Fig. 7b filtered using the BSI = 77 threshold h) Histogram of S2REP which shows the bimodality more clear.

CSI index is generally used as an indicator of crop water stress and can only be retrieved from thermal bands. S2REP is instead a more direct indicator of chlorophyll content and hence can be used to monitor the health and function of crops since chlorophyll is a major regulator of crop health status. It could also be indirectly related to soil water content. However, it has been established that the leaf chlorophyll content decrease is not always caused by a reduction in leaf water content (water stress condition) (Ceccato et al., 2001), as the opposite holds for the case of maize (Schlemmer et al., 2005; Khayatnezhad & Gholamin, 2012), although some maize cultivars can be drought resistant keeping a high chlorophyll content (Khayatnezhad & Gholamin, 2012). On the other hand, the vegetation stress indices due to water deficiency -such as the one used in the current project (CSI)- are not always reliable. The reason for this is that water stress indices of this type are based on the assumption that a plant will minimize transpiration when it is start being depleted of water. In addition, the computation itself might import errors which could come from LAI, emissivity and *Delta*. However, it has been found that there are plant species which cease transpiration in order to maintain water thus preventing water stress conditions (Ceccato et al., 2001). Therefore, those species can wrongly be taken as water stressed. In other words, spectral bands that span from visible to near-infrared, as well as thermal are only suitable for specific

vegetation species regarding their water content, since those bands are commonly used to either of the two approaches (i.e. chlorophyll estimation and transpiration crop stress index).

Furthermore, there are studies that have correlated positively the Red Edge Parameters with the leaf chlorophyll content such as Ding and Zhang (2016). Frampton et al. (2013) in a preliminary study regarding S2 showed that the corresponding REP (S2REP) is highly correlated with Leaf Chlorophyll Concentration (LCC), at least based on the crops that they studied which do not include maize. In the current study it is evident that S2REP contains such extra information through the bimodality which probably is owed to the increased leaf chlorophyll content partly at least (Fig. 7a, f, h). As far as maize concerned, despite a direct correlation between LCC and water content has not been grounded, the leaf spectral reflectance seems to be affected by acute water stress as Schlemmer et al. (2005) observed. The same authors explain this such that transmittance of NIR wavelengths is affected by the air between the cells of the leaf tissue which in turn are related to water content. Therefore, based on this information S2REP could possibly include information about leaf water status in the present project to a certain extent, although without being supported by strong evidence.

As far as the 2-dimensional histogram between CSI and S2REP concern, it suggests that there is almost no correlation between the two variables. This means that the observed S2REP-CSI negative association is extremely weak if not absent, which in turn indicates that S2REP in the current scene is not related to water stress but some other kind of stress. In addition, almost no negative CSI values are observed, which would suggest that there are not well irrigated maize plots, although there might be a computation bias (systematic error) due to *Delta* as mentioned above which could drag the values to the positive side. This must be the most probable reason of the bias since *Delta* is not widely tested and when developed it was based on different crop type (Rodriguez et al., 2005).

In addition, the S2REP- K_C graph (Fig. 7f) shows a positive correlation after BI filtering, even though there is large scattering, and the CSI- K_C (Fig. 7g) shows a negative correlation. The absolute values of the fitted curve slopes on the unfiltered graphs can be seen in Fig. 8a-d below against K_C , which suggest that S2REP slopes are higher than CSI, thus S2REP is better in discriminating crop stressed areas where the assumption of K_C -NDVI stress conditions does not hold since it changes at a higher rate than CSI.

Additionally, the graphs of CWR (Fig. 7d) and NDVI (Fig. 7 e) between L8 and S2 seem to be reasonable, as the relation is a 1:1. The scattering of the data -which is very small compared to the comparisons in the Appendix (App. Fig. 9, 10) and category (a) output (Fig. 6)- could probably owed to transformations and absence of complete harmonization of the two sensors. This suggests that a common AC, accurate co-registration and other adjustments (e.g. spectral and BRDF) are of some importance if one concerns about perfect L8 and S2 matching.

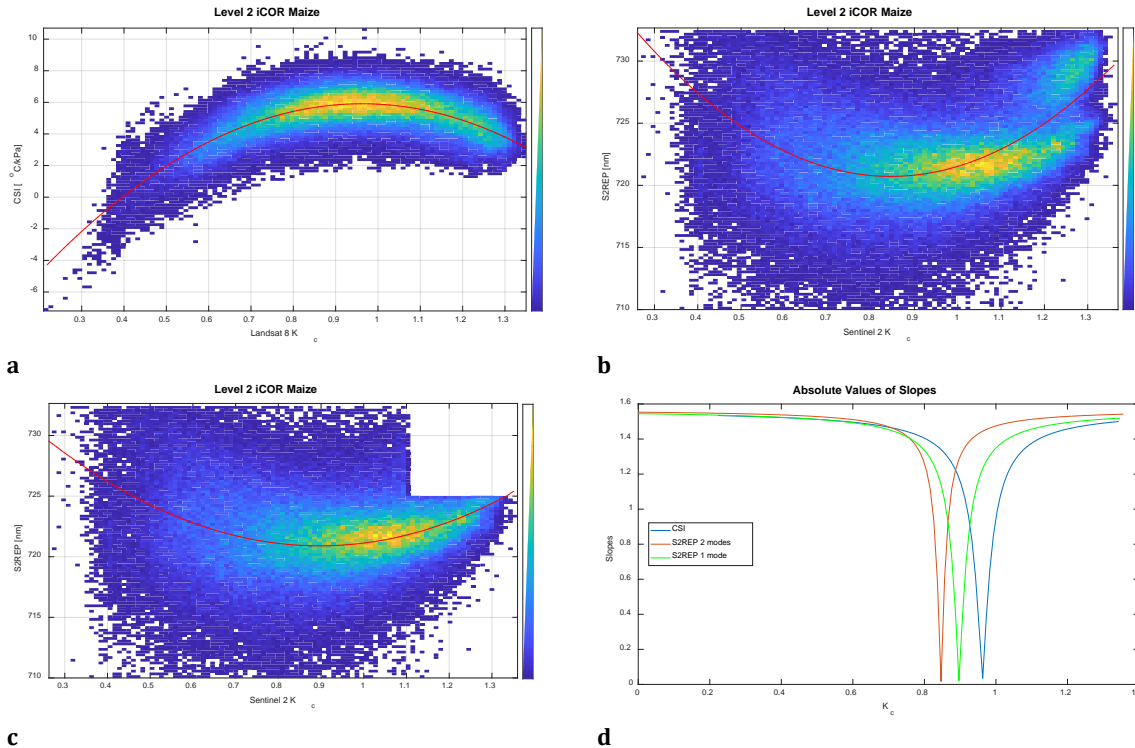


Figure 8: a) threshold $K_c = 0.96$ where slopes is 0 with coefficients of 2nd order polynomial being $a=-18.4$, $b=35.5$, $c=-11.1$ b) threshold $K_c = 0.85$ where slope is 0 with coefficients of 2nd order polynomial being $a=33.8$, $b=-57.3$ and $c=744.9$. Both modes are taken into account for the curve fitting c) threshold $K_c = 0.90$ where slope is 0 with coefficients of 2nd order polynomial being $a=21.5$, $b=-38.6$, $c=738.3$. The second mode has been disregarded from the curve fitting d) Absolute values of slopes for CSI, S2REP using both modes and S2REP using just the one mode as seen in Fig. 8c

4. Conclusions and Suggestions

In conclusion, throughout this project it has been found that the effect the discrepancies of L8 and S2 are important regarding every aspect such as spectral response, AC and mis-registration. Furthermore, since the NDVI cannot depict accurate estimation of CWR under crop stressed conditions S2REP was investigated on how it could potentially show some aspect of crop stress. With the current methodology used, it is found that S2REP could better discriminate between stressed and not stressed crops than CSI being related not only to water content but also to other sources of stress.

Since, officially, the project was supposed to be accomplished under a restricted period of time it is apparent that further work can be conducted in order to enhance and expand the knowledge. In particular, since a combined operational use of Sentinel 2 and Landsat 8 is needed, it is of primal importance that the two datasets are completely harmonized. In other words, it is suggested that the following steps can be followed in the view of the aforementioned; i) an even better parametrized common atmospheric correction based on the iCOR algorithm or another one as suggested by other authors such as Zhang et al. (2018) and Claverie et al. (2017) ii) a more precise co-registration e.g. an area and/or feature based

and/or frequency domain based satellite image co-registration along with geometric correction iii) spectral adjustments. In this way the products will be more homogeneous and, thus, provide a more consistent and reliable time series in the future. Regarding the NDVI weakness to disclose stress information, further research is needed in order to find such information using multispectral datasets, although the weakness is present indeed. Since S2REP is a promising VI regarding crop stress, its use and correlation analysis with K_C could be expanded to a larger number of images in order to minimize the bias that could originate from the specific restricted study area, and in this way could assist the up to now widely used K_C -NDVI method that only holds for standard crop conditions.

5. References

- Akdim, N., Alfieri, M. S., Habib, A., Choukri, A., Cheruiyot, E., Labbassi, K., Menenti, M. 2014. Monitoring of Irrigation Schemes by Remote Sensing: Phenology *versus* Retrieval of Biophysical Variables. *Remote Sensing* 6. 5815-5851.
- Akike, S., Samanta, S. 2016. Land Use/Land Cover and Forest Canopy Density Monitoring of Wafi-Golpu Project Area, Papua New Guinea. *Journal of Geoscience and Environment Protection* 4. 1-14.
- Alfieri, S., M., Menenti, M. 2016. D3.4 In Season Crop water demand package. *Managing crOp water Saving with Enterprise Services*. MOSES project Deliverable 3.4
- Allen, G., R., Pereira, S., L., Raes, D., Smith, M. 1998. FAO Irrigation and Drainage Paper No. 56 Crop Evapotranspiration (Guidelines for computing water requirements). FAO, Water Resources, Development and Management Service. Rome, Italy.
- Allen, R., Tasumi, M. and Trezza, R. 2002. SEBAL (Surface Energy Balance Algorithms for Land)-Advanced Training and User's Manual-Idaho Implementation, Version 1.0
- Berk, A., Anderson, G., P., Acharya, P., K., Bernstein, L., S., Muratov, L., Lee, J., Fox, M., Adler-Golden, S., M., Chetwynd, J., H., Hoke, M., L., Lockwood, R., B., Gardner, J., A., Cooley, T., W., Borel, C., C., Lewis, P., E. 2005. MODTRAN™5, A Reformulated Atmospheric Band Model with Auxiliary Species and Practical Multiple Scattering Options: Update. *Algorithms and Technologies for Multispectral, Hyperspectral, and Ultraspectral Imagery XI, Proceedings of SPIE* 5806. DOI: 10.1117/12.606026
- Calera, A., Campos, I., Osann, A., D'Urso, G., Menenti, M. 2017. Remote Sensing for Crop Water Management: From ET Modelling to Services for the End Users. *Sensors* 17. 1104-1128.
- Ceccato, P., Flasse, S., Tarantola, S., Jacquemoud, S., Gregoire, M., J. 2001. Detecting vegetation leaf water content using reflectance in the optical domain. *Remote Sensing of Environment* 77. 22-33
- Claverie, M., Masek, J., G., Ju, J., Dungan, J., L. 2017. Harmonized Landsat-8 Sentinel-2(HLS) Product User's Guide. Available at: <http://hls.gsfc.nasa.gov/>. Retrieved on: 24/05/2018
- Congedo L. 2016. Semi-Automatic Classification Plugin Documentation. DOI: <http://dx.doi.org/10.13140/RG.2.2.29474.02242/1>
- Di Felice, A., Mazzolena, M., Marletto, V., Spisni, A., Tomei, F., Alfieri, S., M., Menenti, M., Villani, G., Scarpino, G., Battilani, A. 2017. Climate Services for Irrigated Agriculture: Structure and Results from the MOSES DSS. Symposium Società Italiana per le Scienze del clima (SISC), Bologna, Italy. Available at: https://www.researchgate.net/publication/322576756_Climate_Services_for_Irrigated_Agriculture_Structure_and_Results_from_the_MOSES_DSS, Retrieved on: 03/04/2018.
- D'Urso. 2010. Current Status and Perspectives for the Estimation of Crop Water Requirements from Earth Observation. *Ital. J. Agron./ Riv. Agron.* 5. 107-120.
- European Space Agency. (2015). Sentinel-2 User Handbook. Issue 1.2. Available at: https://sentinels.copernicus.eu/web/sentinel/user-guides/document-library/-/asset_publisher/xslt4309D5h/content/sentinel-2-user-handbook
- Filella, I., Penuelas, J. 1994. The red edge position and shape as indicators of plant chlorophyll content, biomass and hydric status. *International Journal of Remote Sensing* 15:7. 1459-1470. DOI: dx.doi.org/10.1080/01431169408954177
- Frampton, J. W., Dash J., Watmough, G., Milton, J. E. 2013. Evaluating the capabilities of Sentinel-2 for quantitative estimation of biophysical variables in vegetation. *ISPRS Journal of Photogrammetry and Remote Sensing* 82. 83-92.

- Gao, F., Masek, J., Wolfe, R., E. 2009. Automated registration and orthorectification package for Landsat and Landsat-like data processing. *Journal of Applied Remote Sensing* 3.
- Idso, S., B., Reginato, R., J., Jackson, R., D., Pinter Jr., P., J. 1981a. Measuring Yield-Reducing Plant Water Potential Depressions in Wheat by Infrared Thermometry. *Irrigation Science* 2. 205-212.
- Idso, S., B. 1981b. Surface Energy Balance and the Genesis of Deserts. *Archives for Meteorology Geophysics and Bioclimatology A*, 30. 253-260.
- Kääb, A., Winsvold, H., S., Altena, B., Nuth, C., Nagles, T., Wuite, J. 2016. Glacier Remote Sensing Using Sentinel-2. Part I: Radiometric and Geometric Performance, and Application to Ice Velocity. *Remote Sens.*, 8(7). 598.
- Khayatnezhad, M., Gholamin, R. 2012. The effect of drought stress on leaf chlorophyll content and stress resistance in maize cultivars (*Zea mays*). *African Journal of Microbiology Research* 6 (12). 2844-2848.
- Rikimaru, A., Miyatake, S. 1997. Development of Forest Canopy Density Mapping and Monitoring Model using Indices of Vegetation, Bare soil and Shadow. *Asian Conference on Remote Sensing (ACRS)*. Available at: <http://a-a-r-s.org/aars/proceeding/ACRS1997/Papers/FR97-5.htm>
- Rocha, J., Perdigao, A., Melo, R., Henriques, C. 2012. Remote Sensing Based Crop Coefficients for Water Management in Agriculture. In: Chapter 8, Sustainable Development –Authoritative and leading edge content for environmental management. ISBN 978-953-51-0682-1.
- Rodriguez, D., Sadras, V., O., Christensen, L., K., Belford, R. 2005. Spatial assessment of the physiological status of wheat crops as affected by water and nitrogen supply using infrared thermal imagery. *Australian Journal of Agriculture Research* 56. 983-993.
- Roy, P., S., Miyatake, S., Rikimaru, A. 1997. Biophysical Spectral Response Modeling Approach for Forest Density Stratification. *Asian Conference on Remote Sensing (ACRS)*. Available at: <http://a-a-r-s.org/aars/proceeding/ACRS1997/Papers/FR97-7.htm>
- Roy, P., S., Sharma, K., P., Jain, A. 1996. Stratification of density in dry deciduous forest using satellite remote sensing digital data-An approach based on spectral indices. *J. Biosci.* 21:5. 723-734.
- Schlemmer, M., R., Francis, D., D., Shanahan, J., F., Schepers, J., S. 2005. Remotely Measuring Chlorophyll Content in Corn Leaves with Differing Nitrogen Levels and Relative Water Content. *Agronomy and Horticulture – Faculty Publications*. 106-112. Available at: <http://digitalcommons.unl.edu/agronomyfacpub/1>
- Skakun, S., Roger, J., C., Vermote, E., F., Masek, J., G., Justice, C., O. 2017. Automatic sub-pixel co-registration of Landsat-8 Operational Land Imager and Sentinel-2A Multi-Spectral Instrument images using phase correlation and machine learning based mapping. *International Journal of Digital Earth*. DOI: 10.1080/17538947.2017.1304586
- Spisni, A., Sapia, L., D., De Bonis, R., Vingione, G., Scarpino, G., Alfieri, S., M., Menenti, M., Gorte, B., Mousivad, A. 2017. D3.1 Crop mapping package. *Managing crop water Saving with Enterprise Services*. MOSES project Deliverable 3.1
- Sterckx, S., Knaeps, E., Adriaensen, S., Reusen, I., Keukelaere, L., D., Hunter, P., Giardino, C., Odermatt, D. 2015. OPERA: AN ATMOSPHERIC CORRECTION FOR LAND AND WATER. *Proc. Sentin. Sci. Work.* 3-6.
- Sterckx, S., Knaeps, S., Kratzer, S., Ruddick, K. 2015. SIMilarity Environment Correction (SIMEC) applied to MERIS data over inland and coastal waters. *Remote Sensing of Environment* 157. 96-110.
- Stumpf, A., Michea, D., Malet, J., P. 2018. Improved Co-Registration of Sentinel-2 and Landsat-8 Imagery for Earth Surface Motion Measurements. *Remote Sensing* 10. 160-179.
- U.S. Geological Survey. (2016). Landsat 8 (L8) Data Users Handbook. Version 2.0. Sioux Falls, South Dakota. Available at: <https://landsat.usgs.gov/landsat-8-l8-data-users-handbook>

Vermote, E., Justice, C., Claverie, M., Franch, B. 2016. Preliminary analysis of the performance of the Landsat 8/OLI land surface reflectance product. *Remote Sensing of Environment* 185. 46-56. doi.org/10.1016/j.rse.2016.04.008

Weng, Q., Lu, D., Schubring, J. 2004. Estimation of land surface temperature-vegetation abundance relationship for urban heat island studies. *Remote Sensing of Environment* 89. 467-483.

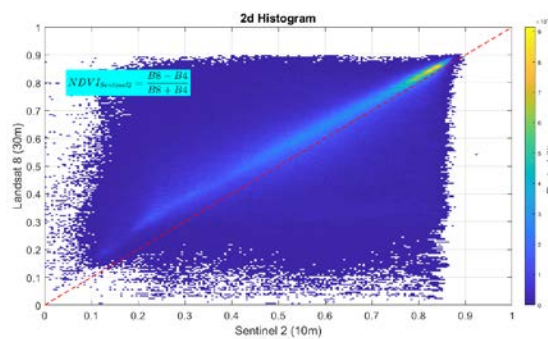
Yan, L., Roy, D., P., Li, Z., Zhang, H., K., Huang, H. 2018. Sentinel-2A multi-temporal misregistration characterization and an orbit-based sub-pixel registration methodology. *Remote Sensing of Environment* 215. 495-506.

Zhang, H., K., Roy, D., P., Yan, L., Zhongbin, L., Huang, H., Vermote, E., Skakun, S., Roger, J., C. 2018. Characterization of Sentinel-2A and Landsat-8 top of atmosphere, surface, and nadir BRDF adjusted reflectance and NDVI differences. *Remote Sensing of Environment* 215. 482-494.

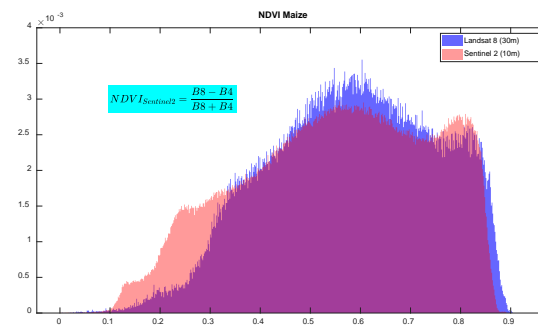
6. Appendix

The graphs as can be seen below have been generated by S2 NDVI computed using B8 instead of B8a (Fig. 9 a-f). By comparing the Fig.9a and Fig. 9d, the impact of the spatial resolution is visible as 30m spatial resolution of both S2 and L8 (Fig. 9d) give a less spread of the data, thus converting products to common spatial resolution gives better results. The atmospheric effect due to water vapor of B8 as U.S. Geological Survey (2016) notes is apparent especially in Fig. 9a and Fig. 9d. By comparing them with Fig. 9g which uses the B8a S2 it suggests that B8 S2 is unsuitable in being used for NDVI calculation since it shows a systematic error, thus the relation NDVI S2-NDVI L8 is far from 1:1. Regarding the absolute differences whose central tendency moments do not accumulate over 0, as well as the large standard deviations they are the effects of the absence of co-registration. The AC that was used is the DOS1 through the Semi-automatic classification Plug-in in QGIS (Congedo, 2016). The discrepancy observed in Fig. 9 j-l is due to both absence of co-registration (spread of data) and differentiation in AC (systematic error in low and high values) of L2 products (LaSRC AC for L8 and sen2cor AC for S2). This can be also justified if one compares the Fig. 9 g-i with Fig. 9 j-l, which shows that there is no systematic error in DOS1, thus the systematic error is owed to ACs and not the absence of co-registration or different spatial resolutions. On the contrary, the impact of spatial resolution can be seen in the comparison between Fig. 10 g-i and Fig. 10 j-l which suggest that the resampling of S2 to L8 spatial resolution (30m) increases the precision.

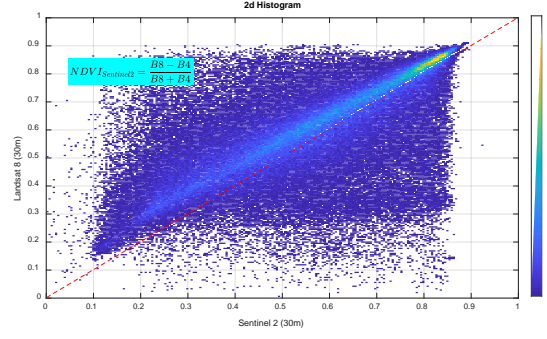
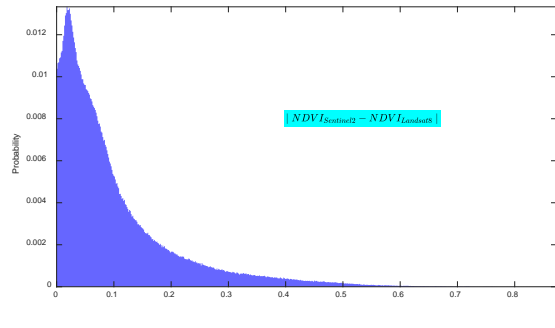
Fig. 10 m-o represents the iCOR comparisons. Taking everything into account the iCOR (Fig. 10 m-o) seems to be slightly better than DOS1 (Fig. 10 j-l) correction based on their summary statistics (central moments). Also there seems to be a difference between the two especially at the lowest and highest values (Fig. 10 p-u). Namely, DOS1 underestimates the high values and overestimates the low values compared to iCOR. However, in the current work iCOR was considered to be more accurate due to the nature of the AC algorithms it uses which are not solely image-based as DOS1, thus could give slightly more realistic values.



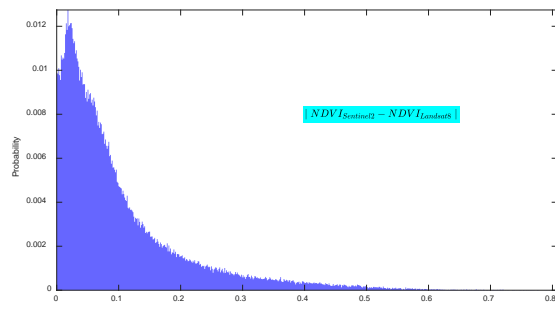
a



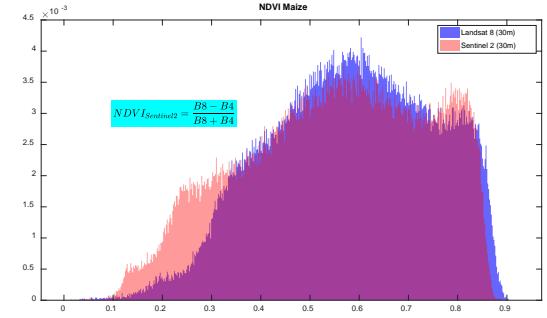
b



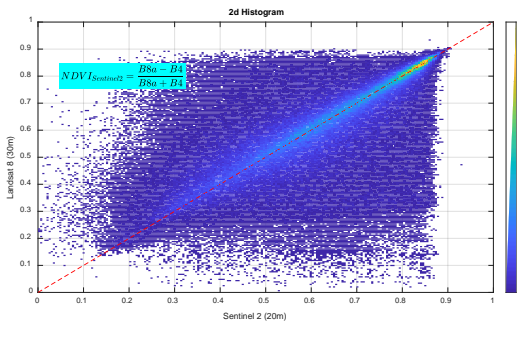
c



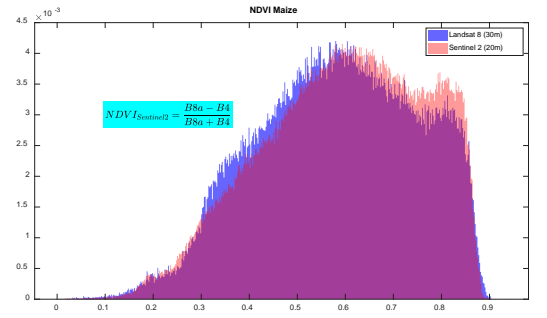
d



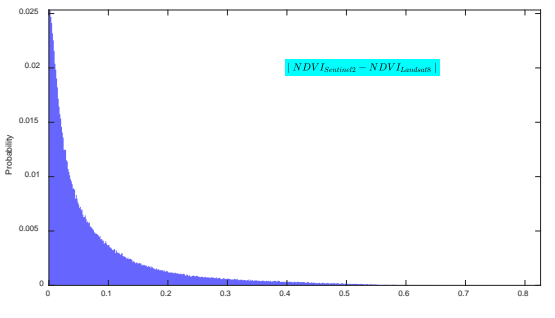
e



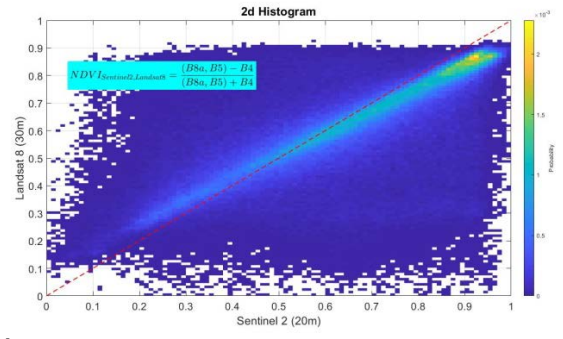
f



g

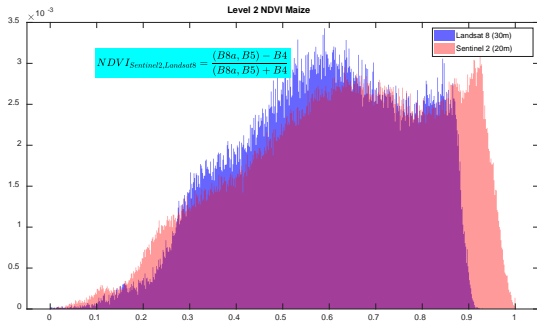


h

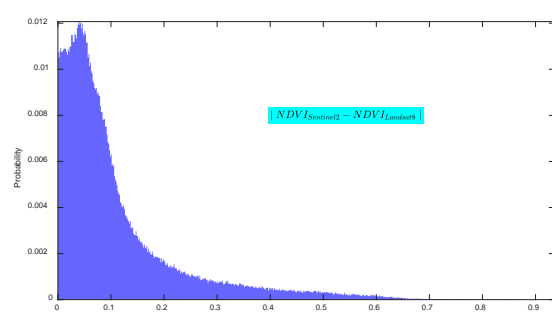


i

j



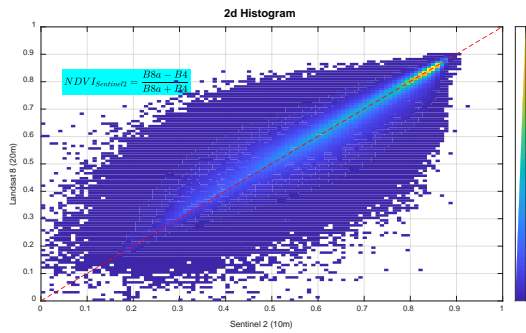
k



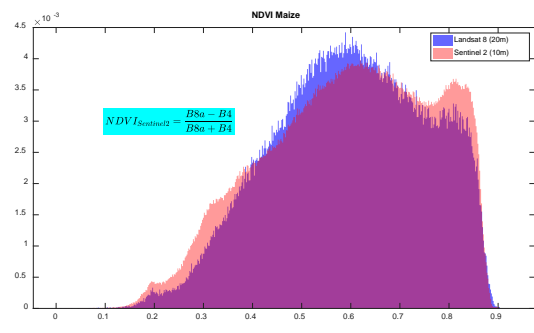
l

Figure 9: a-c) S2 (10m) vs L8 (30m) NDVI (using S2 B8) using DOS1 AC with no co-registration d-f) S2 (30m) vs L8 (30m) NDVI (using S2 B8) using DOS1 AC with no co-registration g-i) S2 (20m) vs L8 (30m) NDVI (using S2 B8a) using DOS1 AC with no co-registration j-l) S2 (20m) vs L8 (30m) NDVI (using S2 B8a) using L2 products with sen2cor and LaSRC ACs respectively, with no co-registration

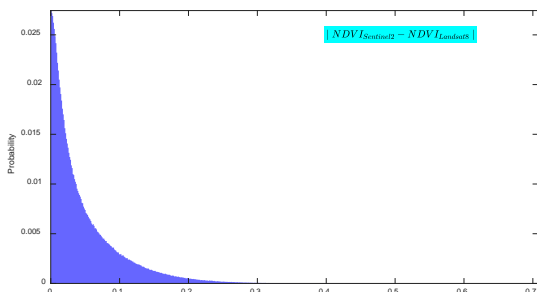
The graphs below (Fig. 10 a-l) represent comparisons with the use of co-registration (reprojection/resampling and collocation SNAP tool) combinations and DOS1 AC, as well as comparison with iCOR AC (Fig. 10 m-u).



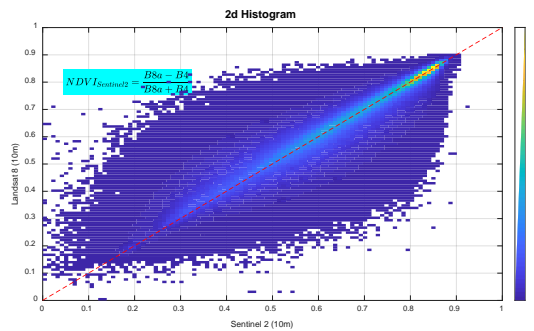
a



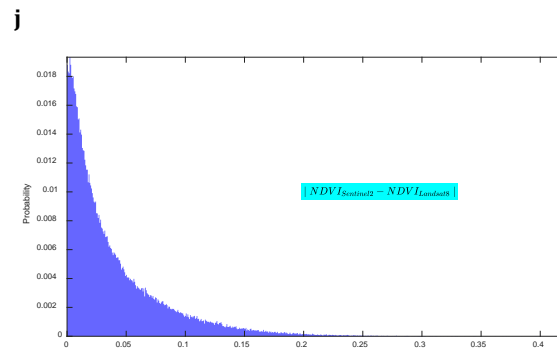
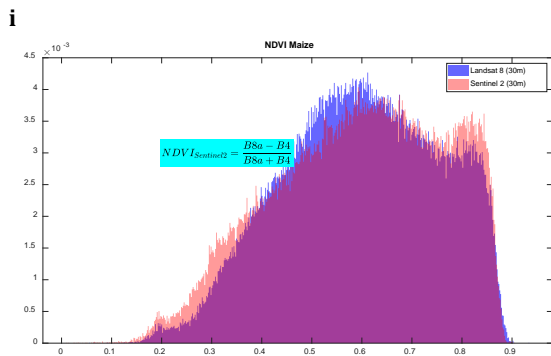
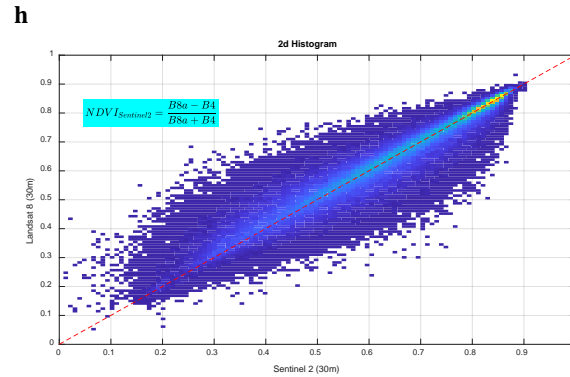
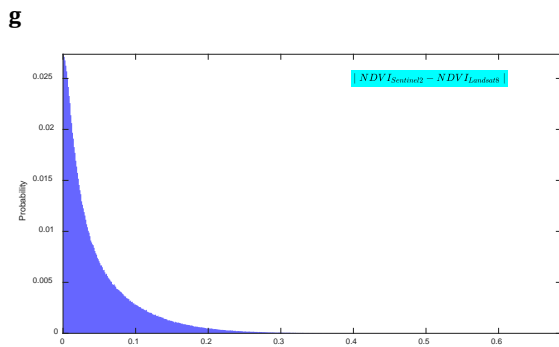
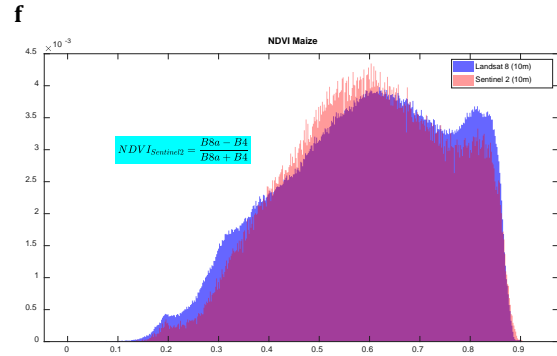
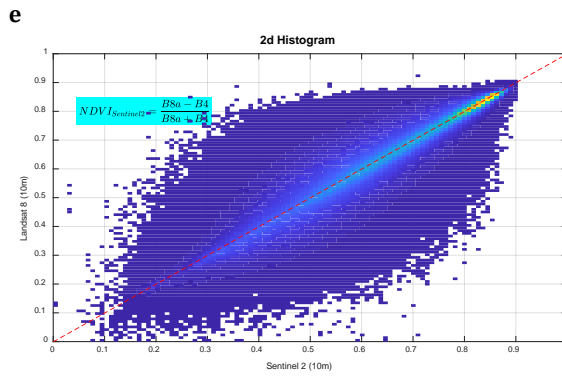
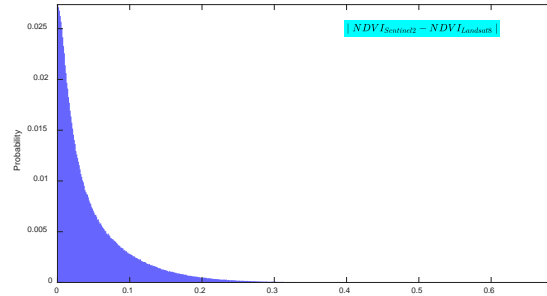
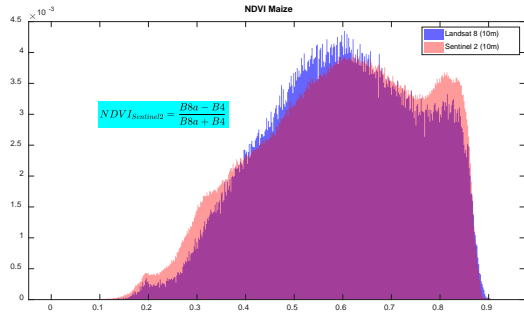
b



c

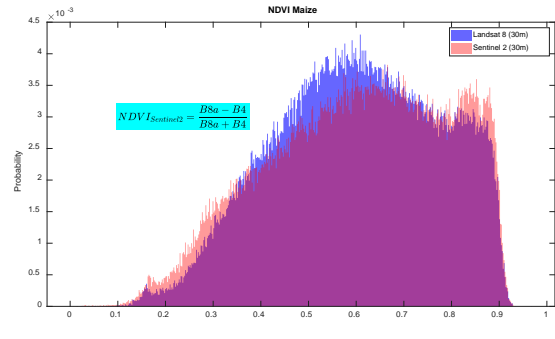
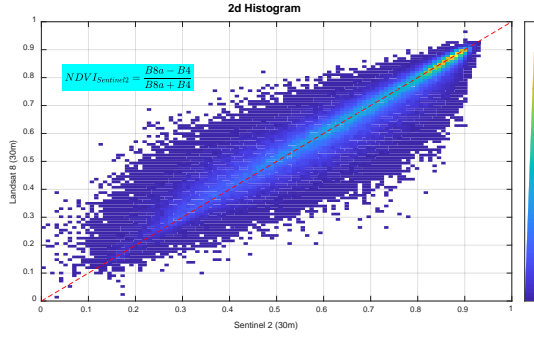


d

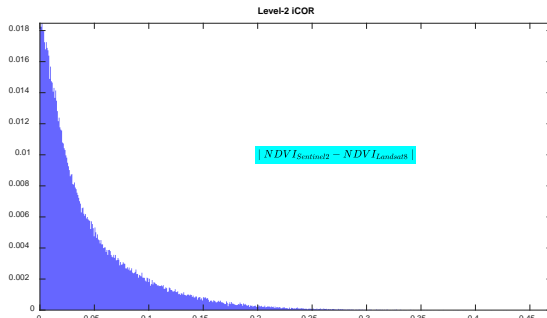


k

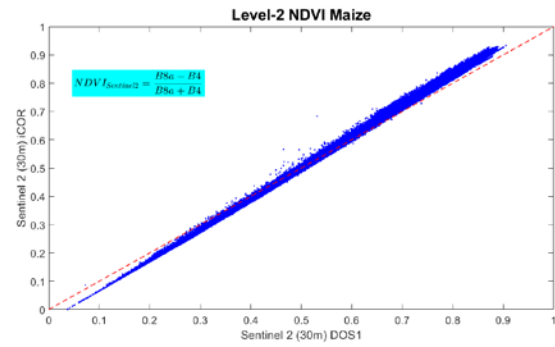
l



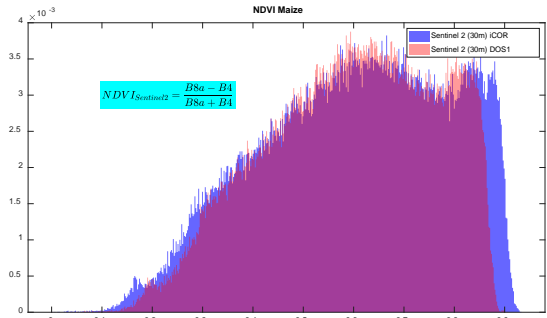
m



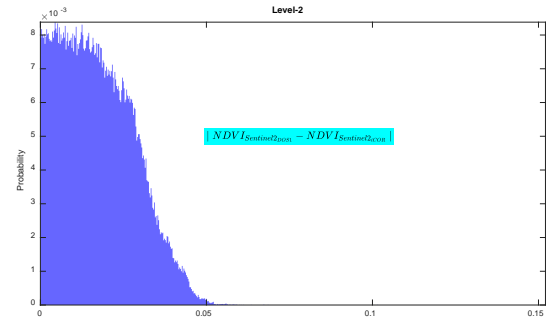
n



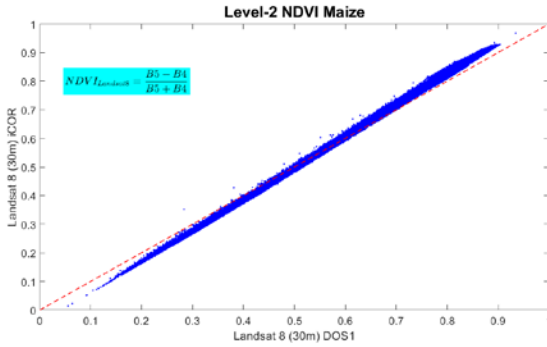
o



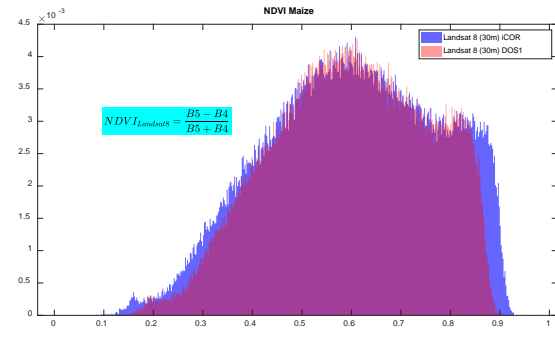
p



q

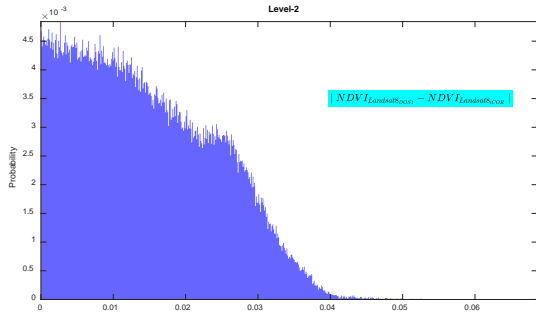


r



s

t



u

Figure 10: a-c) L8 (20m) vs S2 (10m) DOS1 AC, reprojected and resampled in SNAP d-f) L8 (10m) vs S2 (10m) DOS1 AC, reprojected and resampled in SNAP g-i) L8 (10m) vs S2 (10m) DOS1 AC, collocated in SNAP j-l) L8 (30m) vs S2 (30m) DOS1 AC, collocated in SNAP m-o) L8 (30m) vs S2 (30m) iCOR AC, collocated in SNAP p-r) S2 DOS1 vs iCOR AC graphs s-u) L8 DOS1 vs iCOR AC graphs